JEPPD Journal of Endometriosis and Pelvic Pain Disorders

Original Research Article

Development of a domestic animal model for endometriosis: Surgical induction in the dog, pigs, and sheep

Journal of Endometriosis and Pelvic Pain Disorders
1–12

DOI: 10.1177/2284026518773942
journals.sagepub.com/home/pev
SAGE

Emy E Varughese[1], Gregg P Adams[1], Carlos EP Leonardi[1], Pritpal S Malhi[2], Paul Babyn[3], Mary Kinloch[4] and Jaswant Singh[1]

Abstract

Background: Endometriosis affects one in ten women of reproductive age but it is diagnosed at advanced stages. Our objective was to develop a domestic animal model that would permit sequential assessment of endometriotic changes.

Materials and methods: Surgical transplantation of endometrial tissue and fat (n = 4 grafts/tissue/animal) was done in dogs (n = 5), pigs (n = 4), and sheep (n = 5). Autologous grafts were sutured to the visceral (urinary bladder in dogs and pigs and uterus in sheep) and parietal peritoneum. Sham surgeries were performed (dogs and sheep n = 5 and pigs n = 3) by placing fat grafts alone. Plasma estrogen and progesterone concentration was performed prior to surgery and weekly following surgery until euthanasia. Animals were euthanized between 80 and 110 days after surgery. Gross and histopathologic features of endometriotic lesions were recorded.

Results: A variety of lesions from transplanted endometrial grafts included endometriotic cysts, vesicles, solid lesions, or absence of lesions. The proportion of cysts was greater ($p < 0.01$) in dogs (18/20 grafts) than in pigs (5/16) and sheep (5/20). The area of endometriotic lesions at the time of euthanasia was greater than at the time of surgery in dogs ($0.89 \pm 0.11\ cm^2$ vs $0.50 \pm 0.09\ cm^2$; $p < 0.05$), whereas, the size of lesions decreased ($p < 0.05$) by half or more in pigs and sheep. In dogs, endometrial cysts were characterized by simple cuboidal/columnar epithelium, endometrial glands, stromal tissue with hemorrhage and/or hemosiderin-laden macrophages, and smooth muscle cells.

Conclusion: The development of endometriotic cysts was apparent in dogs than in sheep and pigs. Therefore, dog is a better domestic animal model for endometriosis.

Keywords

Animal models, dogs, endometriosis, endometriotic cyst, endometrium, pigs, sheep

Date received: 11 October 2017; accepted: 6 April 2018

Introduction

Endometriosis is defined as the presence of endometrial glands and stroma in ectopic locations, primarily the pelvic peritoneum, ovaries, and rectovaginal septum.[1] It is believed that retrograde reflux of endometrial fragments from the uterus into the peritoneal cavity via oviduct (fallopian tube) results in growth at ectopic sites.[2,3] Although 90% of women with patent oviducts have blood in the peritoneal cavity,[4] endometriosis has a prevalence rate of 10%,[5] indicating that not all women with endometrial fragments in the peritoneal cavity will develop the disease. One of the possible reasons for development of endometriotic lesions in some but not all women is perhaps inefficient functioning of the immune and/or phagocytic system.[6,7]

[1]Department of Veterinary Biomedical Sciences, Western College of Veterinary Medicine, University of Saskatchewan, Saskatoon, SK, Canada
[2]CiToxLAB, Laval, QC, Canada
[3]Department of Medical Imaging, College of Medicine, University of Saskatchewan, Saskatoon, SK, Canada
[4]Medical Faculty, University of Saskatchewan and Saskatoon Health Region, Saskatoon, SK, Canada

Corresponding author:
Jaswant Singh, Department of Veterinary Biomedical Sciences, Western College of Veterinary Medicine, Saskatoon, SK S7N 5B4, Canada.
Email: jaswant.singh@usask.ca

Table 1. Dose, type, and method of administration of drugs used for premedication and induction of anesthesia and post-operative analgesia (body weight (BW)).

Species	Premedication (intramuscular)	Induction of anesthesia (intravenous)	Post-operative analgesia (intramuscular)
Dogs	Hydromorphone[a] (0.1 mg/kg BW) and acepromazine[b] (0.02–0.04 mg/kg BW; depending on temperament of the dogs)	Diazepam[f] (0.25 mg/kg BW) and ketamine (5 mg/kg BW) via cephalic vein	Hydromorphone (0.05 mg/kg BW)
Pigs	Butorphanol[c] (0.2 mg/kg BW), xylazine[d] (1 mg/kg BW), and ketamine[e] (5 mg/kg BW)	Xylazine (1 mg/kg BW) and ketamine (2 mg/kg BW) via ear vein ± induction via masking with isoflurane if required	Butorphanol (0.2 mg/kg BW)
Sheep	Butorphanol (0.2 mg/kg BW) and xylazine (0.2 mg/kg BW)	Diazepam (0.25 mg/kg BW) and ketamine (5 mg/kg BW) via jugular vein	Butorphanol (0.2 mg/kg BW)

BW: body weight.
[a]Hydromorphone Hydrochloride Injection USP, Sandoz, Canada.
[b]Atravet, Boehringer Ingelheim, Burlington, Ontario, Canada.
[c]Torbugesic, Ayerst Laboratories, Montreal, Canada.
[d]Rompun, Bayer Inc, Toronto, Canada.
[e]Vetalar, Bioniche Animal Health Canada Inc, Belleville, Ontario, Canada.
[f]Diazepam Injection USP, Sandoz, Canada.

Interactions between endometrial components and serosal surfaces have been studied in vitro using whole explants of the peritoneum and endometrium from uterine tissue collected from women undergoing surgical procedures[8] or using shed menstrual effluent.[9] Such in vitro models provide useful information regarding the characteristics of initial attachment between the endometrium and serosal surface but fail to provide information regarding long-term tissue interactions. Ethical and practical constraints prevent study of the pathogenesis and progression of endometriosis in women; therefore, several animal models have been used to better understand the disease. Women and non-human primates are the only species to undergo menstruation at the time of endometrial shedding and to develop spontaneous endometriosis.[10] Despite the advantages associated with using non-human primates as models, they are expensive to maintain, and it is ethically sensitive to carry out invasive experiments in these animals.[11] Induction of endometriosis has been attempted by injection of endometrial fragments into the peritoneal cavity or by surgical transplantation of endometrium onto organs in the peritoneal cavity in mice,[12,13] rats,[14] and rabbits.[15] Small laboratory animals are cost-effective, but they develop lesions that are small and difficult to identify,[11] making them less suitable as models for sequential studies. Furthermore, the use of immuno-deficient mice confounds the investigation of immuno-regulatory component involved in the pathogenesis of the disease.[16] Therefore, there is a need for a suitable animal model that develops macroscopically visible lesions characteristic of endometriosis in women which will enable repeated and sequential imaging for diagnostic and treatment trials.

Domestic species (e.g. dogs, pigs, and sheep) as models for endometriosis have not been reported. Therefore, the objectives of this study were: (1) to surgically induce endometriosis and characterize endometriotic lesions in these three species, and (2) to compare the characteristics of lesions with previously described lesions in women to determine the most suitable animal model.

Materials and methods

Animals

Surgeries were performed in dogs (mixed-breed Husky; n = 10; body weight = 15–20 kg; age = 2–4 years), pigs (mixed breed; n = 8; body weight = 100–110 kg; age = 7 months–1 year post puberty), and sheep (Suffolk; n = 10; body weight = 80–90 kg; age = 1–2 years). Sheep and pigs were assigned randomly to an endometrial transplant group (sheep n = 5 and pigs n = 4) or sham surgery group (sheep n = 5 and pigs n = 4). Dogs were assigned to groups (n = 5 each in treatment and control group) by randomized block design based on exfoliative vaginal cytology; proestrus (n = 2) and anestrus (n = 3) in the endometrial transplant group, and proestrus (n = 1), diestrus (n = 1) and anestrus (n = 3) in the sham group. The animal procedures were approved by the University Committee on Animal Care and Supply, and the Animal Research Ethics Board, University of Saskatchewan (AUP Protocol No. 20140026).

Surgery

Dogs, pigs, and sheep were fasted for 12, 24, and 48 h, respectively, before surgery. Animals were pre-medicated for surgery, anesthesia induced by intravenous injection (dose and drugs described in Table 1), intubated, and maintained under general anesthesia with isoflurane (Isoflurane USP, Pharmaceutical Partners of Canada Inc, Richmond Hill, Ontario, Canada).

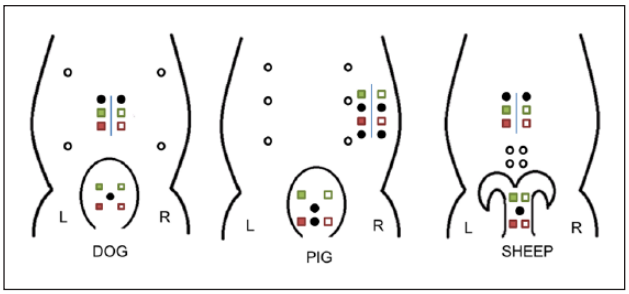

Figure 1. Dorsoventral view of abdomen showing the site of incision (line) in relation to mammary glands (teat shown as open circles) in dogs, pigs, and sheep. Endometrial tissue (red) and fat tissue (green) were sutured on the dorsal aspect of the urinary bladder (dogs and pigs) or uterus (sheep) and on the abdominal wall on either side of incision. Only fat grafts were sutured at the respective sites in the sham group. Grafts were placed with either epithelial side contacting the peritoneal surface (clear boxes; right side) or the non-epithelial (stroma and glands) side contacting the peritoneal surface (solid boxes; left side). Plastic beads (solid circles) served as markers for imaging and postmortem examination.

The ventral abdomen was shaved and aseptically prepared for laparotomy. A 7.5–10 cm-long median incision was made 7.5 cm caudal to the umbilicus in dogs and 7.5–10 cm cranial to the udder in sheep. A right paramedian incision was used in pigs approximately 7.5–10 cm dorsolateral to the mammary glands, at the level of the 5th–7th teats. Unilateral hysterectomy of the left uterine horn was performed in the treatment group. The excised uterine horn was opened longitudinally and the endometrium was carefully separated from the remaining tissue and dissected into small pieces (approximately 1×0.5 cm in dogs, and 2×1 cm in pigs and sheep), and the epithelial (lumen side) and non-epithelial sides were identified. Fat (for making control tissue grafts) was dissected from the falciform ligament (dogs) or lateral ligaments of the urinary bladder (sheep and pigs), and serosal (lumen side) and non-serosal sides were identified. Endometrial and fat grafts were sutured onto the parietal peritoneum (ventral abdominal wall on either side of the incision) and visceral peritoneum (caudodorsal aspect of the urinary bladder in dogs and pigs, caudodorsal aspect of the uterus in sheep; Figures 1 and 2) using 4–0 absorbable suture material (PDS*II, Ehicon Inc, Mexico city, Mexico). The uterus was chosen as the site of grafting in sheep, as the urinary bladder was difficult to access from the abdominal opening. The fat graft was placed immediately cranial to the endometrial graft at each site. To examine the effect of contact surface, tissue grafting on the left side was done with non-epithelial side of endometrium and non-serosal side of fat in contact with the peritoneum and those on the right side involved contact between the epithelial side of endometrium and the serosal lining of fat grafts with the peritoneum. Plastic jewelry beads (4 mm diameter) were sutured adjacent to the grafted tissues using 4–0 non-absorbable material (Novafil, Covidien IIc, Mansfield, MA, USA) and served as markers during imaging and at postmortem examination (Figures 1 and 2). The surgical procedure and site of graft placement for the sham group were identical to the treatment group but only fat grafts were used. In brief, two fat grafts were sutured onto the visceral peritoneum (urinary bladder in dogs and pigs and uterus in sheep) with a plastic bead between grafts. Two fat grafts were placed on the parietal peritoneum, one on either side of ventral incision with a bead cranial to the graft. The fat graft on the left and right side was placed with the non-serosal side and serosal side, respectively, facing the peritoneum. In addition to serving as sham controls, these animals were used as control group to assess the effect of endometrial grafts on plasma levels of estrogen and progesterone.

In both treatment and sham groups, the sizes (length and width) of grafts were measured before closing the abdomen. The linea alba and subcutaneous tissue were closed in a simple continuous manner using absorbable suture material (PDS*II, Ehicon Inc, Mexico; No. 0/2-0 in dogs, No. 1/2 in pigs, and No. 0/1 in sheep). The skin was closed using non-absorbable suture material (Covidien IIc, Mansfield, MA, USA; No. 2-0 Novafil in dogs and 0 Monosof in sheep and pigs).

Post-operative analgesics (Table 1) were administered in animals that showed signs of pain. All animals recovered uneventfully except one pig in the treatment group which developed an abdominal hernia. A second corrective surgery was performed to reduce the herniated mass, but the pig was euthanized due to extensive adhesions. Skin sutures were removed after 14 days or after complete healing of the incision site. None of the animals developed any complications related to daily activities such as feeding and voiding during the study period.

Blood sampling and hormone measurements

Blood samples were collected in 10 mL heparinized tubes (Becton and Dickinson Vacutainer Systems, Franklin Lakes, NJ, USA) immediately prior to surgery and then weekly for 13 weeks (dogs), 5 weeks (pigs), or 12 weeks (sheep). Samples were centrifuged at 1500*g* for 20 min, and plasma stored at −20°C for later radioimmunoassay (RIA).

Plasma estrogen concentration was measured using a previously described RIA procedure.[17] The intra-assay coefficients of variation for low- and high-reference samples were 11% and 7.3%, respectively. The inter-assay coefficients of variation for low- and high-reference samples were 12.5% and 11.6%, respectively. Plasma progesterone concentration was measured using a commercial RIA kit (ImmuChem Progesterone^{125} kit, ICN Pharmaceuticals, Inc, Diagnostic Division, Costa Mesa, CA, USA). The intra- and inter-assay coefficients of variation were 10.8% and 1.7%

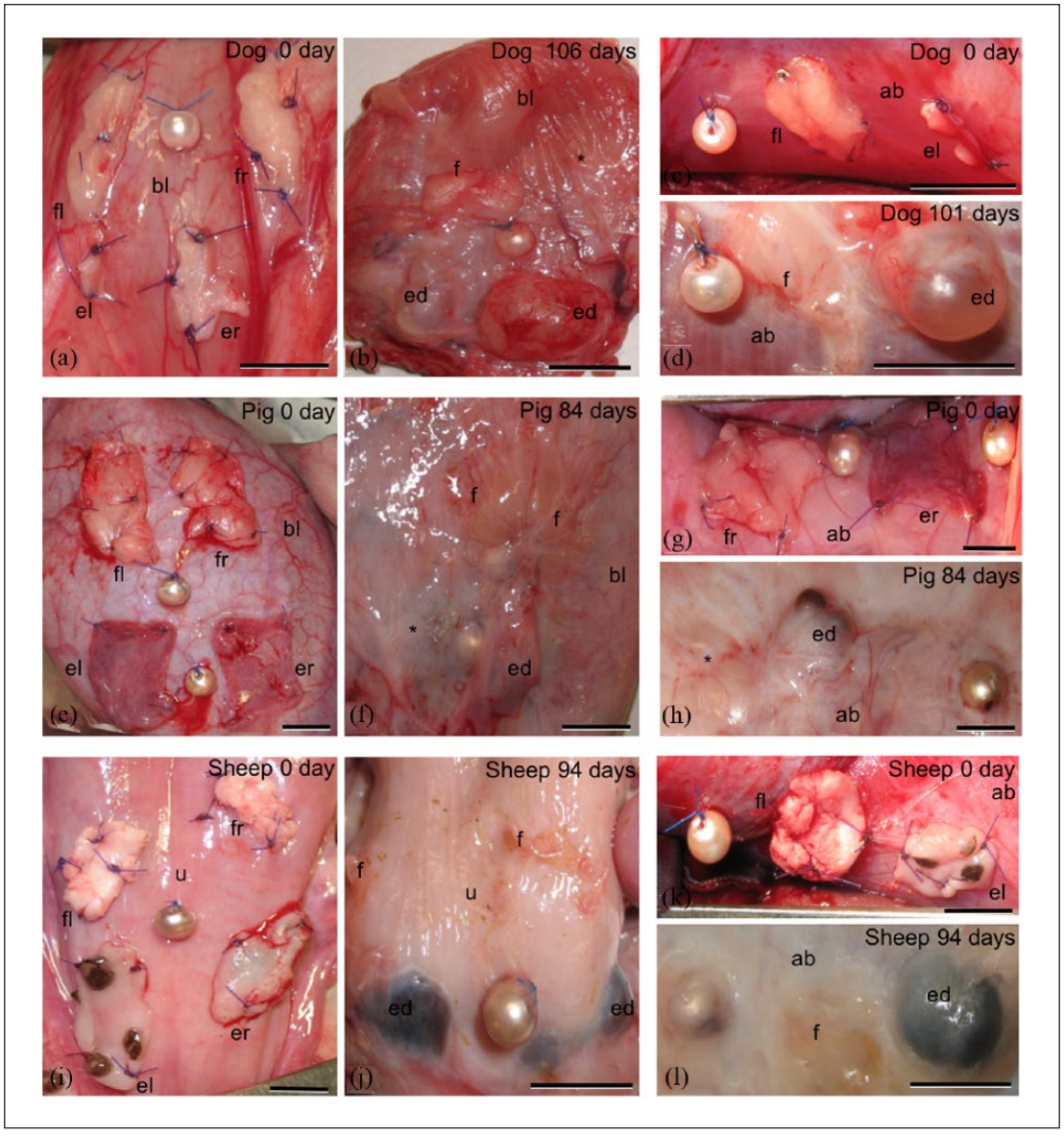

Figure 2. Endometrial and fat grafts at the time of surgical transplantation (a, c, e, g, i and k) and lesions post-surgery (b, d, f, h, j and l; at the time of euthanasia) in dogs (a–d), pigs (e–h), and sheep (i–l) on the serosal surface of visceral peritoneum (dorsal wall of urinary bladder in a, b, e and f and dorsal wall of uterus in i and j) and parietal peritoneum (dorsal surface of abdominal wall in c, d, g, h, k and l). Species and days post-surgery are indicated at the upper right corner of each figure. Plastic jewelry beads were sutured as markers. A variety of lesions including endometriotic cysts {b, d, f (right), h, j, l}, vesicles, solid lesions, and absence of lesions {f (left)} was noticed. Fat was either seen as remnants {b (left), d, f, j, l} or absence of lesion {b (right), h}. Scale bar = 1 cm; ab: abdomen; bl: urinary bladder; ed: endometriotic cyst; el: left endometrial graft; er: right endometrial graft; f: remnants of fat; fl: left fat graft; fr: right fat graft; u: uterus; *absence of lesion.

and 11.1% and 6.5%, respectively, for low- and high-reference samples.

Gross and histologic assessment of grafted tissues

Except for the five control dogs, that were re-used later for another experiment, animals were euthanized between 80 and 110 days post-surgery to permit gross and histologic examination of the transplant sites. Control group dogs (n = 5) were used as treatment dogs in another experiment for which they underwent a second surgery between 150 and 180 days. The data from previous sham surgery was recorded during the second surgery. Euthanasia was accomplished by intravenous administration (cephalic vein in dogs, ear vein in pigs, and jugular vein in sheep) of sodium pentobarbital (1 mL/5 kg body weight; euthanyl forte, Bimeda-MTC Animal Health Inc, Cambridge, Ontario, Canada). Dogs and pigs were pre-medicated (Table 1) prior to euthanasia. The abdominal wall was reflected, and all

Table 2. Surgical transplantation of the endometrial tissue and fat (n = 4 grafts/tissue/animal) was done in dogs (n = 5), pigs (n = 4), and sheep (n = 5). Autologous grafts were sutured to the visceral (urinary bladder in dogs and pigs and uterus in sheep) and parietal peritoneum (abdominal wall). Types of endometriotic lesions on the left (stromal side of endometrium in contact with serosa) and right (epithelial side of endometrium in contact with serosa) side of serosal surface of visceral and parietal peritoneum were recorded that showed solid lesions (s), cysts (c), vesicles (v), or no detectable lesion (n). Pre-fixed number indicated the number of grafts that exhibited the given morphology.

Species	Pareital peritoneum		Visceral peritoneum	
	Left	Right	Left	Right
Dog	5c	5c	4c and 1s	4c and 1n
Pigs	2c and 2s	2c, 1v, and 1s	1v, 2s, and 1n	1c and 3s
Sheep	1c, 2v, 1s, and 1n	1c, 3v, and 1n	1c, 2s, and 2n	2c, 2s, and 1n

graft sites were identified by relative position from the plastic beads. The dimensions of the grafts were measured using a measuring scale. Lesions were excised and fixed in 4% paraformaldehyde for 24–48 h.

For histologic evaluation, tissues were embedded in paraffin, sectioned at a thickness of 5 µm, and placed on poly-L-lysine–coated glass slides. Hematoxylin and eosin (H&E) staining was used for routine analysis of all sections (modified from Culling[18]). Staining techniques using Masson's trichrome stain (to differentiate between cellular components and connective tissue) and Periodic acid–Schiff (PAS) stain (to detect basement membrane) was performed by a commercial laboratory (Prairie Diagnostic Center, Western College of Veterinary Medicine, Saskatoon, Saskatchewan, Canada) on selected sections (n = 2) from dog lesions that had cells/structures that appeared different. Evaluation of the tissue sections was performed using light microscopy (Olympus BX41TF, Tokyo, Japan). Evaluation of autofluorescence was performed using confocal laser scanning microscopy (Leica, TCS SP5, Germany).

Scanning electron microscopy

In order to examine the microscopic features of the lining epithelium of cystic lesions, a subset of samples from dogs (n = 2 lesions) were processed for scanning electron microscopy. Briefly, tissue samples (fixed in 4% paraformaldehyde) were dehydrated in increasing concentrations of ethanol; ethanol was substituted with 50% and 75% amyl acetate (v/v in ethanol; 15 min each) followed by three changes in 100% amyl acetate; tissues were critical-point-dried in liquid carbon dioxide (1200 psi pressure setting in Polaron E3000; Polaron, Watford, England) and finally coated with gold in a sputter coater (Edwards S150B, Edwards Co., England). Samples were examined using Hitachi SU8000 Scanning electron microscope at an accelerating voltage of 1.5 kV.

Statistical analysis

The size (area) of the graft at the time of surgery versus the time of euthanasia (for both endometrial and fat grafts placed on bladder/uterus or abdomen) was compared using paired t-tests (SPSS Inc, USA). Values are reported as mean ± SEM unless otherwise specified. Probability (p) values of ≤ 0.05 were considered significant, whereas those between >0.05 and ≤ 0.10 were considered tendencies approaching significance.

Results

Gross assessment of transplanted tissues

The gross appearance of grafted tissues at the time of surgery and at the time of euthanasia several weeks later is shown in Figure 2. Fluid-filled structures ≥1 cm were defined as cysts and those <1 cm were defined as vesicles. All but one of the endometrial tissue grafts (19 of 20 grafts) in dogs developed into endometriotic lesions with single or multiple cysts (Figure 2(b) and (d); Table 2). Endometrial grafts in pigs (Figure 2(f) and (h)) and sheep developed into solid lesions, vesicles, cysts (Figure 2(j) and (l); Table 2), or no detectable lesion (Table 2). The proportion of cystic lesions was greater ($p < 0.01$) in dogs (18/20) than in pigs (5/16) and sheep (5/20). The proportion of successful transplantations (endometrial grafts that developed into endometriotic lesions) and those with cystic lesions did not differ ($p > 0.05$) between the left (non-epithelial side touching peritoneum) and the right (epithelial side touching peritoneum) sides of surgeries in dogs, pigs, or sheep (Table 2). There was no difference ($p > 0.05$) in proportions of successful tissue grafts on visceral versus parietal peritoneum in dogs (10/10 vs 10/10), pigs (7/8 vs 8/8), or sheep (7/10 vs 8/10). Fat tissue grafts in treatment and control group dogs (8/20 and 6/20, respectively), and sheep (9/20 and 9/20) were seen as remnants or were completely undetectable (Figure 2(b), (d), (j), and (l)), whereas some fat grafts in pigs were well preserved (11/16 in treatment group and 7/12 in control group) while the remaining were undetectable (Figure 2(f) and (h)).

Adhesions between abdominal wall grafts and mesentery were observed in all dogs given endometrial transplants (5/5) but only in one in the sham group (1/5; $p = 0.04$).

Table 3. Surgical transplantation of endometrial tissue and fat (n = 4 grafts/tissue/animal) was done in treatment dogs (n = 5), pigs (n = 4), and sheep (n = 5). Autologous grafts were sutured to the visceral (urinary bladder in dogs and pigs and uterus in sheep) and parietal peritoneum (abdominal wall). Control group animals (n = 5 dogs, 3 pigs, and 5 sheep) had only fat grafts (last four columns). Data were compared between size (cm^2; mean ± SEM) of endometrial and fat grafts transplanted on visceral and parietal peritoneum at the time of surgery (S) and 3 months post-surgery (PS; at euthanasia) in the treatment group.

Species	Treatment group								Control group			
	Endometrial grafts (cm^2)				Fat grafts (cm^2)				Fat grafts (cm^2)			
	Visceral peritoneum		Parietal peritoneum		Visceral peritoneum		Parietal peritoneum		Visceral peritoneum		Parietal peritoneum	
	S	PS	S	PS	S	PS	S	PS	S	PS	S	PS
Dogs	0.46±0.08	1.09±0.18**	0.54±0.17	0.70±0.12	0.64±0.19	0.09±0.06**	0.60±0.12	0.31±0.09*	1.25±0.19	0.35±0.15**	1.02±0.18	0.04±0.04*
Pigs	1.45±0.08	0.42±0.11**	1.52±0.19	0.64±0.14**	1.50±0.12	0.76±0.17**	1.63±0.12	0.28±0.12**	2.17±0.48	1.42±0.11*	2.00±0.25	0.25±0.35**
Sheep	1.53±0.15	0.29±0.08**	1.11±0.08	0.45±0.11**	1.37±0.09	0.41±0.17**	1.13±0.12	0.15±0.08**	1.93±0.23	0.33±0.09**	0.93±0.04	0.06±0.04**

S: surgery; PS: post surgery.
*$p < 0.05$, **$p < 0.01$.

One dog (1/5) in the treatment group had adhesions between graft on urinary bladder (right endometrial graft) and cervix. An equal number of treatment (2/4) and control group (2/3) pigs developed adhesions between the intestinal mesentery (mostly jejunum) and the incision site, and one (1/4) had adhesions between the broad ligament of uterus and the urinary bladder. All sheep in the treatment group (5/5) had varying degrees of adhesion between the uterus, grafts, and the mesentery, whereas 2/5 sheep in the sham group developed adhesions between grafts and mesentery ($p = 0.16$). Combined among graft sites (visceral and parietal peritoneum) and species, a greater proportion of surgical sites had adhesions in the treatment versus sham group (12/14 vs 5/13; $p < 0.02$). Combined among species and treatment groups, the proportion of surgical sites with adhesions was greater for parietal versus visceral peritoneum (12/19 vs 7/19; $p < 0.01$).

The area of grafted tissues (length x width) at the time of surgery and endometriotic lesions at the time of euthanasia are listed in Table 3. There was no difference ($p > 0.05$; t-test) between size of left and right grafts/lesions on bladder/uterus and abdomen in dogs, pigs, and sheep either at the time of surgery or at 3 months after surgery; therefore, data from the left and right grafts/lesions were combined to obtain mean sizes.

In dogs, endometriotic lesions on serosal surface of the urinary bladder were more than double the size compared to endometrial grafts transplanted at surgery ($p = 0.005$; paired t-test). Cystic lesions on abdominal wall followed a similar pattern (i.e. became larger) although not statistically significant different than at the time of surgery ($p = 0.21$). Overall (combined between urinary bladder and abdominal grafts), the size of endometriotic lesions at 3 months post-surgery was larger ($0.89 \pm 0.11\ cm^2$) compared to endometrial grafts at the time of surgery ($0.50 \pm 0.09\ cm^2$) in dogs. Fat grafts were either seen as remnants or were not detectable and shrunk in size ($p < 0.05$) in both treatment and control group dogs. In pigs and sheep, the size of endometrial lesions decreased by half or more ($p < 0.05$) by 3 months post-surgery. Fat grafts in treatment and control group also decreased in size ($p < 0.05$) in both pigs and sheep.

Histological characterization of endometriotic lesions

Histological characteristics of lesions in different species are illustrated in Figures 3–5.

In dogs, irrespective of stage of estrous cycle at the time of surgery and site of transplantation (bladder versus abdomen), endometriotic lesions contained single or multiple cysts of varying sizes (Figure 3(a) and (b)) with clear-serous, serosanguinous or sanguineous fluid. The wall of the cyst was composed of lining epithelium, endometrial glands, smooth muscles, and stromal tissue (Figure 3(c) and (d)) surrounded by the mesothelial cells (facing the peritoneal cavity). The lining epithelium of cysts varied from simple squamous-cuboidal to low/high cuboidal (Figure 3(e)), cuboidal-columnar or columnar epithelium (Figure 3(g)). Apical surface of cuboidal/columnar cells was lined by varying number of short microvilli (Figure 3(c) inset). There were papillary projections into the lumen and infoldings of the lining epithelium (Figure 3(f)) in some cysts. Intraepithelial glands (Figure 3(g)) were seen in the lining epithelium as well. Cytoplasmic changes like stratified squamous metaplasia with keratinization (Figure 4(a)) and ciliated epithelium were observed in the lining epithelium of few cysts. Cyst luminal contents consisted of white blood cells (WBC; neutrophils, lymphocytes, and macrophages), red blood cells (RBC), sloughed epithelial cells, and/or secretion. There was considerable vascularization of the cyst (Figure 3(e)). Normal, dilated (Figure 4(b)) and cystic (Figure 4(c)) endometrial glands were seen in the wall of the cysts. Some dilated and cystic endometrial glands also contained WBC, RBC, sloughed epithelial cells, and/or secretions. Varying amount of smooth muscle

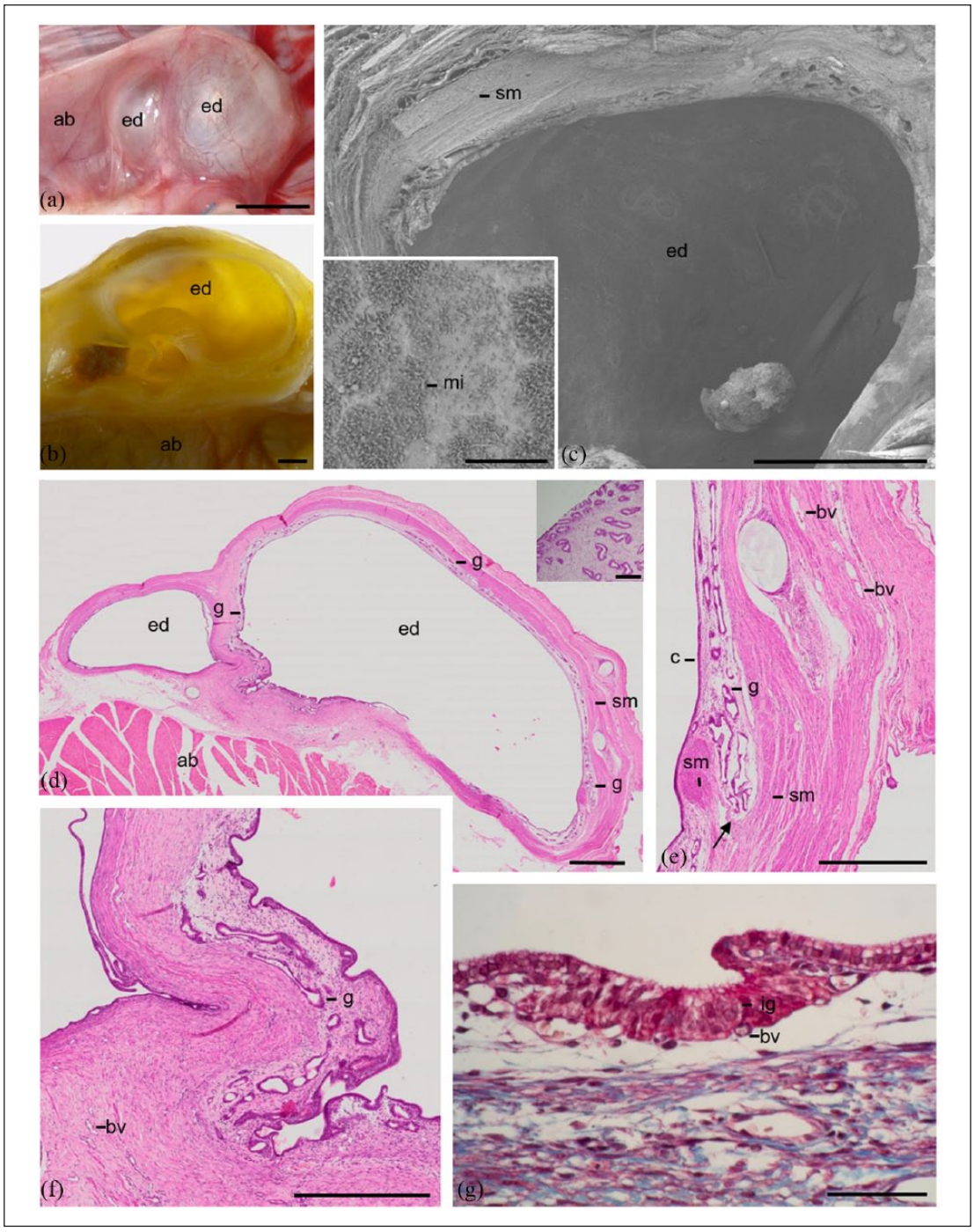

Figure 3. Histopathological features of endometriotic cyst in a dog. Right endometrial graft developed into multiple endometriotic cysts 105 days post-surgery at the time of euthanasia (a) external appearance in fresh lesion; (b) cross-section through the cysts after tissue fixation, transmitted light. (c) Scanning electron microscopy of the cyst cavity show smooth surface of the cyst lined with cells having short microvilli and hexagonal borders (inset). (c) There is also a projection into the cavity. (d) Histological section of the lesion shows an endometriotic cyst and vesicle on the abdomen surrounded by endometrial glands. Inset shows number of glands present at surgery in endometrium. Note that a considerable number of glands surround the cyst at euthanasia. Low cuboidal/columnar epithelium (e, f and g) with occasional intraepithelial glands (g) was seen lining the cysts with endometrial stromal and glandular cells surrounding the cyst (e and f). A well-defined layer of smooth muscle was seen surrounding the cyst (e). (e) Invasion of endometrial glands (arrow) through smooth muscle. Cyst had infoldings and projections within the cyst wall (d and f) and was vascularized with capillaries closely associated with epithelium (g). ((d)–(f), H&E staining and bright-field microscopy), (g) Masson's trichrome staining (epithelium and cells, red; collagen fibers, blue). ab: abdomen; bv: blood vessel; ed: endometriotic cyst; c: cuboidal epithelium; g: endometrial glands; ig: intraepithelial glands; mi: microvilli; sm: smooth muscle fibers; v: vesicle. Scale bars: (a) = 1 cm, (b)–(d) = 1 mm, Inset in (c) = 5 µm, Inset in (d) = 200 µm, (e) and (f) = 500 µm, (g) = 50 µm.

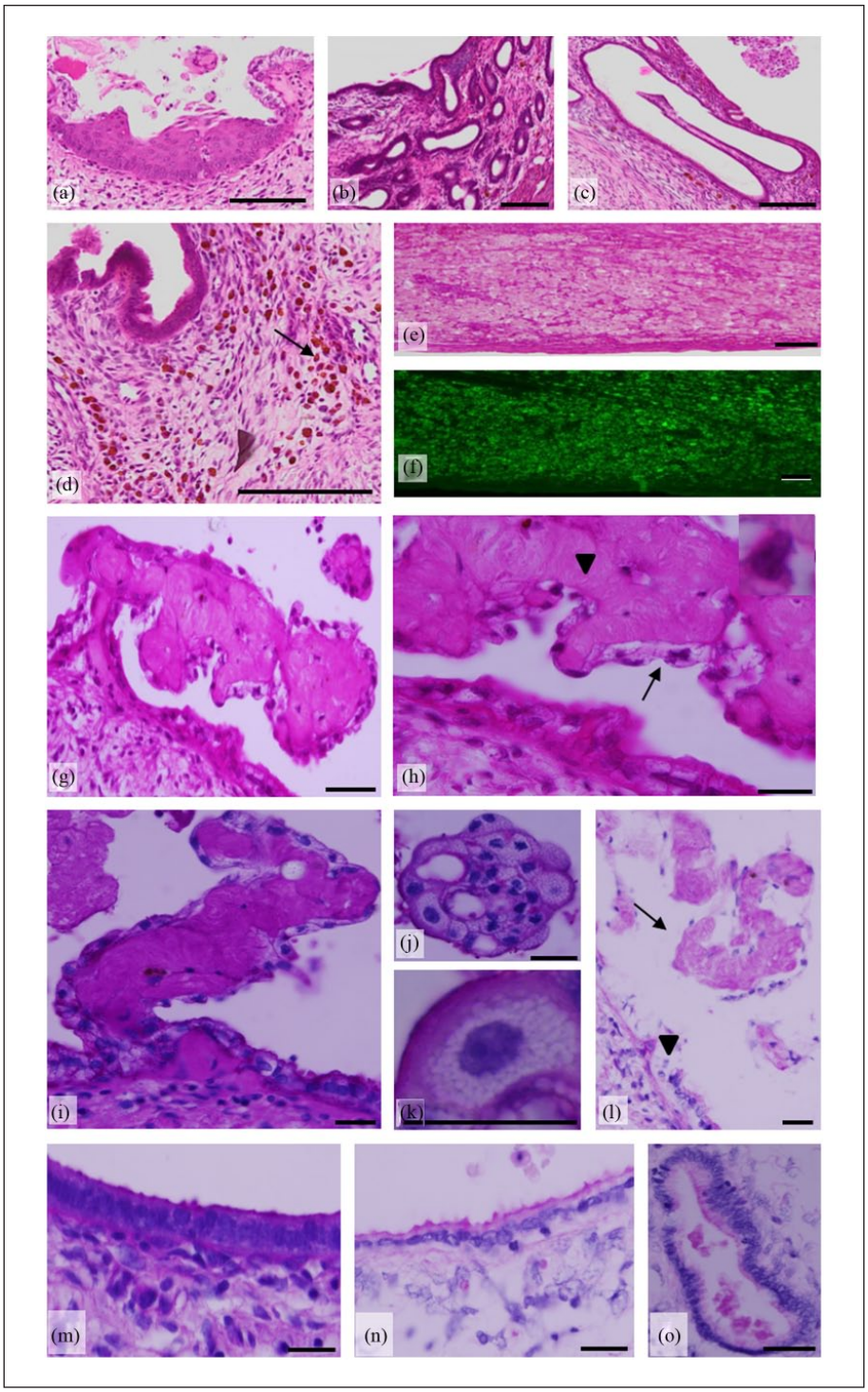

Figure 4. Histomorphological characterization and identification of cytoplasmic and neoplastic changes in endometriotic cyst of a dog. Squamous metaplasia with keratinization of epithelial lining of cyst in one dog (a); normal, dilated (b), and cystic glands (c) in the wall of cysts; evidence of stromal bleeding (d) with numerous hemosiderin-laden macrophages (arrow); pseudoxanthoma cells (e) that were autofluorescing (f); and papillary projections (g) from the wall of a cyst lined by simple cuboidal epithelial cells (h) with abundant bubbly/foamy cytoplasm (arrow), irregularly shaped nucleus with nuclear atypia (two prominent nucleoli; inset) and hyalinized papillary core (arrowhead). PAS staining showing papillary projection (i) and clusters of sloughed off epithelial cells in the lumen of a cyst (j) with bubbly/foamy cytoplasm and nuclear atypia with prominent nuclei (k). PAS with diastase digestion cleared out glycogen from the cytoplasm of epithelial cells lining papillae (arrow) and the some parts of lining epithelium (arrowhead) of cyst (l); other parts of lining epithelium of cyst wall did not get cleared following digestion ((m) without digestion and (n) with digestion) indicating the presence of mucin. Epithelial cells of some endometrial glands also stained for mucin and contained mucinous secretory products within the lumen (o). (a)–(h), H&E staining, (i)–(k), (m) PAS staining; (l), (n), (o) PAS staining after diastase digestion; scale bars: (a)–(f) = 100 µm, (g) = 50 µm, (h)–(o) = 20 µm.

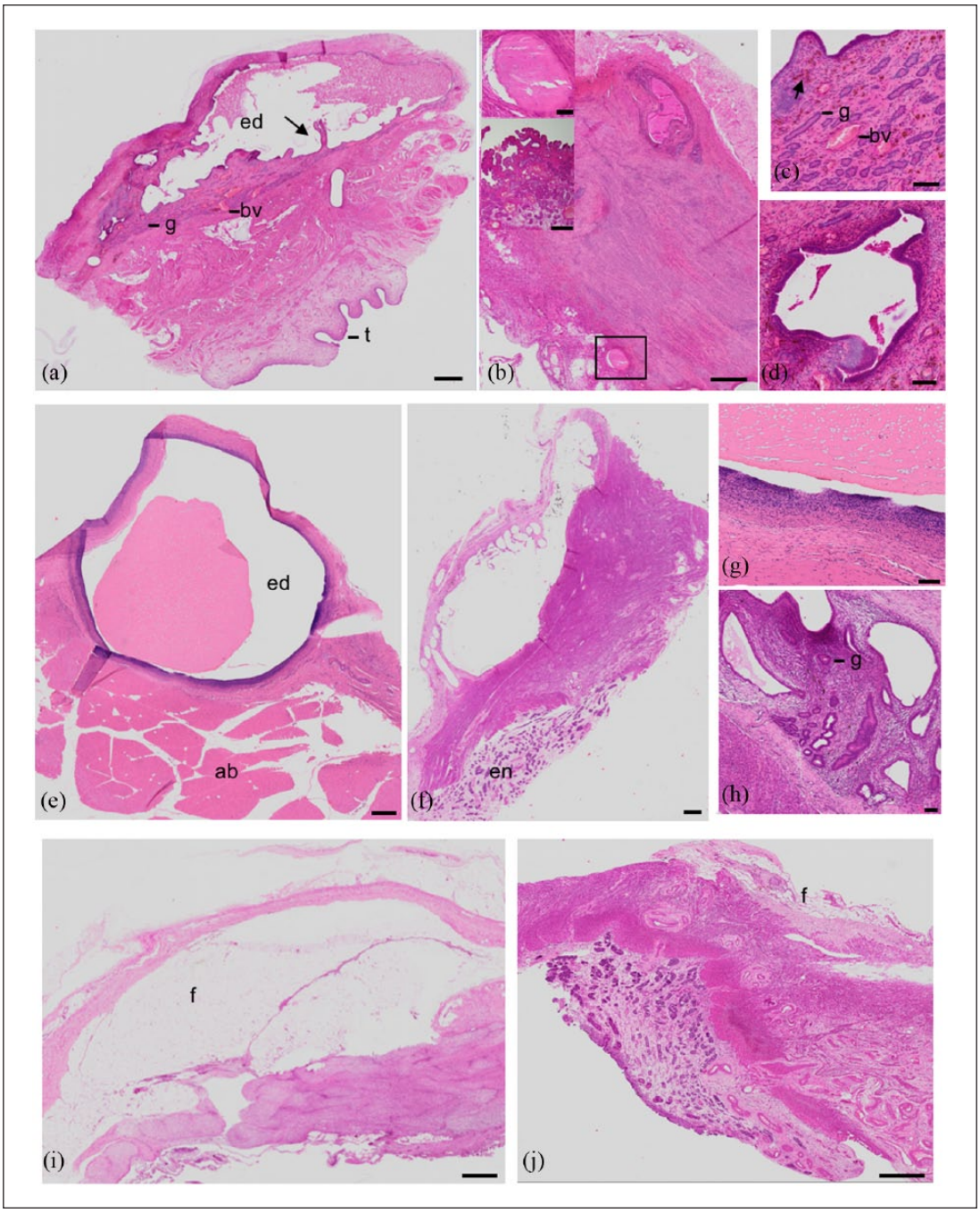

Figure 5. Histopathology of endometriotic lesions/cysts in pigs and sheep. Cyst on the urinary bladder in pigs lined by cuboidal epithelium, surrounded by glands and blood vessels, filled with blood and papillary projections (arrow) protruding into the lumen of the cyst (a), blood-filled dilated gland surrounded by normal glands. First inset (area indicated by square) shows osseous metaplasia. Second inset shows number of glands present in endometrium at surgery. Note that there is considerable reduction in number of glands in lesions at euthanasia (b), Normal glands interspersed with numerous blood vessels (c; arrow indicates hemosiderin-laden macrophages), and cystic glands (d) were seen in the cyst wall of pigs, endometriotic cyst on parietal peritoneum in sheep with no glands in cyst wall (e), cyst on the serosal surface of uterus in sheep with absence of glands. Note the number of glands in endometrium (en) of uterus seen below compared to no glands in lesion (f), pink eosinophilic secretion within lumen of cyst (h), Normal, dilated, and cystic glands seen in very few endometriotic lesions in sheep. Notice pink secretory products within lumen of cystic gland on the extreme left (h), well preserved (i) and remnants of fat (j) in pigs and sheep, respectively of the control group. ab: abdomen; bv: blood vessel; ed: endometriotic cyst; en: endoemtrium; f: remnants of fat; g: endometrial glands; t: transitional epithelium of urinary bladder. Scale bars: (a, b, e, f, I and j) = 0.5 mm, (c, d, g and h) and 1st inset in (b) = 0.05 mm, and 2nd inset in (b) = 0.2 mm.

fibers surrounded the cysts through which endometrial glands were seen invading (Figure 3(e)), both in parietal and visceral peritoneal grafts. Smooth muscle fibers were either organized in a layer or were scattered in the wall. Stromal bleeding was evident with numerous hemosiderin-laden macrophages (Figure 4(d)). Numerous pseudoxanthoma cells (Figure 4(e)) having autofluorescence (Figure 4(f)) were seen surrounding the cyst wall of abdominal endometrial graft in one dog.

Stage of estrous cycle brought about normal physiological changes in endometrium of uterus that were seen on histology. Similar physiological changes were also seen in endometriotic cysts including secretory changes in endometrial glands and lining epithelium of cysts with respect to high progesterone during diestrous phase or increased vascularity during proestrous-estrous phases.

In one of the five treatment group dogs, endometriotic cyst had epithelial, papillary (vascular) projections (Figure 4(g)) from the cyst wall. These papillae had a hyalinized papillary core (Figure 4(h) and (i)) lined with a single layer of high cuboidal epithelial cells (Figure 4(h) and (i)). The epithelial cells had foamy/bubbly cytoplasm (Figure 4(j)), irregularly shaped nucleus with nuclear atypia (irregularly shaped nucleus and prominent nucleoli; Figure 4(k)). Some of these epithelial cells were also seen as groups scattered within the lumen of the cyst (Figure 4(j)). PAS with digestion cleared out glycogen from the cytoplasm of epithelial cells lining papillae and some areas of lining epithelium of cyst (Figure 4(l)). However, some areas of epithelium lining the cyst wall (Figure 4(m)) and some of the secretory products within endometrial glands contained mucin (Figure 4(n) and (o)), that is, not cleared with PAS digestion. Atypical hyperplasia (enlarged, rounded, irregularly shaped nuclei, and prominent nucleoli) was also seen in endometrial glands (Figure 4(o)).

In pigs, cysts were lined by cuboidal/columnar epithelium with a few papillary projections (Figure 5(a)). Cyst luminal contents consisted of numerous RBC and few WBC. Dilated (Figure 5(b)), normal (Figure 5(c)), and cystic endometrial glands (Figure 5(d)) were seen, but they were fewer (Figure 5(b)) compared to dogs. Stromal bleeding with hemosiderin-laden macrophages (Figure 5(d)) and hemorrhage was observed. Hyperplasia without atypia was observed in few glands. Degeneration of endometrial glands and lining epithelium was also seen. Fibrosis of the incision site with osseous metaplasia (Figure 5(b) inset) was common in areas where abdominal grafts were transplanted.

In sheep, cysts (Figure 5(e) and (f)) were lined by simple cuboidal-columnar epithelium. Cyst luminal contents consisted of pink eosinophilic secretion (Figure 5(g)), numerous RBC, and few WBC.

No papillary projections were observed. Very few endometrial glands (Figure 5(h)) were observed with some lesions having no glands (Figure 5(e)). Dilated glands, if present, were lined by cuboidal epithelium with few RBC and WBC. Hemosiderin-laden macrophages, hemorrhage, and melanin (melanocytes are normally present in sheep caruncular areas) were observed. Degeneration of cyst lining epithelium was also seen.

In the control group of dog, pigs (Figure 5(i)), and sheep (Figure 5(j)), areas of fat grafts consisted of normal adipocytes with no tissue changes.

Concentration of plasma estrogen and progesterone

The stage of the estrous cycle at the time of surgery was unknown for the sheep and pigs. Based on stage of estrous cycle, plasma levels of estrogen and progesterone for dogs were compared. The formation of endometriotic lesions was comparable ($p > 0.05$) between stages of estrus cycle in treatment dogs and between treatment and control dogs.

Discussion

Our objective was to develop a domestic animal model for endometriosis that is suitable for performing sequential and repeated examinations to assess the efficacy of diagnostic imaging procedures and treatments. Surgical induction of endometriosis was carried out in dogs, pigs, and sheep. Evidence of growing endometriotic cysts in dogs with histological characteristics similar to those described in ovarian endometriotic cysts in women[19] led us to conclude that using dogs is the most promising domestic animal model for testing imaging probes and therapy agents for the diagnosis and treatment of endometriosis.

Lesions in dogs developed into endometriotic cysts, whereas cysts, vesicles, and solid lesions were seen in pigs and sheep. Development of similar endometriotic cysts and solid masses has been observed in laboratory animals like rat and rabbit after surgical grafting.[20–22] Although cysts in pigs and sheep contained the classical features of lesions seen in endometriosis, there were fewer or no glands (normal/dilated/cystic) in most lesions with evidence of epithelial and glandular degeneration compared to dogs.

In laboratory animal studies, either complete uterine wall[22] or endometrial layer[21] was used for transplantation. Our study design allowed direct comparison of ability of uterine surface epithelium versus endometrial gland/stromal components in establishing the initial adhesion and further developing into lesions on serosal surface of visceral and parietal peritoneum. Majority of endometrial grafts in dogs developed into cysts regardless whether the epithelial or non-epithelial surface faced the serosal surface of peritoneum. Similar results were obtained in pigs and sheep.

Luminal content of cysts was filled with RBC and WBC, which indicated an inflammatory response by the

body. However, the surrounding cells (stroma and glands) did not undergo cell death, appeared healthy, and there was no major evidence of active inflammatory cell infiltration in the cyst walls. Similar hypothesis is proposed as one of the main reasons for development of endometriosis in women.[23] Cysts in dogs were encapsulated by thick wall (fibrous capsule with or without smooth muscle layer) which could have limited the escape of luminal contents leading to formation of large cysts. In contrast, peritoneal lesions in women appear as red, black, or white lesions based on the extent of vascularization and age of lesion, red being an initial vascularized lesion and white corresponding to an aged, devascularized lesion.[24,25] Conversely, ovarian endometriosis in women is usually characterized by endometriotic cysts lined by endometrial-type epithelium, with endometrial glands (inactive or proliferative type with or without hyperplasia). Cysts in dogs were similar to ovarian endometriotic cysts in women. Further development of the dogs model need to focus on devising an experimental procedure for inducing surface (flat) form of peritoneal endometriosis and to test responsiveness of endometriotic cysts to phases of reproductive cycle and to hormones such as estradiol and progesterone. We postulate that with an increase in post-grafting period and/or change in the size of endometrial grafts, other forms of endometriosis can be induced in the dog model.

Furthermore, epithelial atypia such as squamous metaplasia, stratification, and pleomorphic or hyperchromatic nuclei observed in the lining of ovarian endometriotic cysts in women are most often due to local inflammation but can also be neoplastic.[26] Similar epithelial atypia such as squamous differentiation and mucinous changes were observed in the epithelial lining of cysts in dogs. Mucinous changes are usually associated with atypia, with columnar cells having basal nuclei and abundant pale supranuclear cytoplasm that contains mucin.[27] Secondary changes occurring in lesions due to bleeding or fibrosis can transform areas of endometriosis into granulation tissue with numerous histiocytes also called pseudoxanthoma cells which contain ceroid (degradation products of blood) capable of autofluorescing.[19,28] Similar pseudoxanthoma cells were found in the cyst wall of one dog. Movement of endometrial gland and/or stroma leaving the well-defined endometrium was observed in a few lesions which could indicate invasive capability of endometrial components. Further evaluations by euthanasia after a longer period of time (8–9 months) could help in assessing if cysts retain these characteristics or undergo secondary changes due to bleeding and fibrosis. Another intriguing finding was preliminary evidence of pathologic features resembling clear cell carcinoma (papillary pattern and clear cell type). Such carcinomas are frequently (58%) associated with endometriosis and endometriotic cysts in women.[29,30] The cytoplasm of clear cells is usually described as clear or bubbly[30] due to the presence of glycogen.[31] The clear cells in our study also had similar morphology and contained glycogen, not mucin. These findings also strengthen our model; however, further work would be needed to assess pre-neoplastic potential of endometriotic cysts in dogs by possibly prolonging the duration of the study.

In conclusion, surgical transplantation of endometrium was successful in dogs, pigs, and sheep: however, consistent development of endometriotic lesions was only observed in dogs. Development of a greater proportion of growing endometriotic cysts in dogs with classic combination of endometrial stroma, glands and evidence of hemorrhage and/or hemosiderin-laden macrophages within cysts compared to sheep and pigs led us to conclude dogs as the most suitable domestic animal model for endometriosis among the three species tested. Lesions in dogs are fairly large and easily identifiable. The scope of dog as a deep infiltrating endometriosis model may require placing grafts for a longer duration which requires further study. The dog model can be used for repeated and sequential medical imaging such as ultrasonography, positron emission tomography-computed tomography (PET-CT), and magnetic resonance imaging (MRI) for diagnostic and treatment trials and therefore have significant advantage over laboratory animal models.

Acknowledgements

The authors thank Eiko Kawamuram from the Western College of Veterinary Medicine (WCVM) Imaging Center and Ian Shirley from Department of Veterinary Pathology, WCVM, Canada for their expertise in imaging. They would like to acknowledge the constant guidance of Susan Cook and Kim Tran of the Endocrine Laboratory at Veterinary Biomedical Sciences, WCVM, Canada in the estimation of estrogen and progesterone. They would also like to thank Lawrence Araujo, Kylie Beck, Jessica Nicoletti, Rodrigo Carassco, and Fahrid Huanca for their help in various stages of the research.

Declaration of conflicting interests

The author(s) declared no potential conflicts of interest with respect to the research, authorship, and/or publication of this article.

Funding

The author(s) disclosed receipt of the following financial support for the research, authorship, and/or publication of this article: This research was supported by a grant from the Sylvia Fedoruk Canadian Center for Nuclear Innovation, Canada.

References

1. Burney RO and Giudice LC. Pathogenesis and pathophysiology of endometriosis. *Fertil Steril* 2012; 98(3): 511–519.
2. Sampson JA. Perforating hemorrhagic (chocolate) cysts of the ovary: their importance and especially their relation to pelvic adenomas of endometrial type (adenomyoma of the uterus, rectovaginal septum, sigmoid, etc.). *Arch Surg* 1921; 3: 245–323.

3. Sampson JA. Peritoneal endometriosis due to menstrual dissemination of endometrial tissue into the peritoneal cavity. *Am J Obstet Gynecol* 1927; 14: 422–469.
4. Halme J, Hammond MG, Hulka J, et al. Retrograde menstruation in healthy women and in patients with endometriosis. *Obstet Gynecol* 1984; 64(2): 151–154.
5. Eskenazi B and Warner ML. Epidemiology of endometriosis. *Obstet Gynecol Clin North Am* 1997; 24(2): 235–238.
6. Somigliana E, Vigano P, Gaffuri B, et al. Modulation of NK cell lytic function by endometrial secretory factors: potential role in endometriosis. *Am J Reprod Immunol* 1996; 36(5): 295–300.
7. Vigano P, Gaffuri B, Somigliana E, et al. Expression of intercellular adhesion molecule (ICAM)-1 mRNA and protein is enhanced in endometriosis versus endometrial stromal cells in culture. *Mol Hum Reprod* 1998; 4(12): 1150–1156.
8. Witz CA, Monotoya-Rodriguez IA and Schenken RS. Whole explants of peritoneum and endometrium: a novel model of the early endometriosis lesion. *Fertil Steril* 1999; 71(1): 56–60.
9. Witz CA, Allsup KT, Montoya-Rodriguez IA, et al. Culture of menstrual endometrium with peritoneal explants and mesothelial monolayers confirms attachment to intact mesothelial cells. *Hum Reprod* 2002; 17(11): 2832–2838.
10. D'Hooghe T, Bambra CS, De Jonge I, et al. The prevalence of spontaneous endometriosis in the baboon (Papio anubis, Papio cynocephalus) increases with the duration of captivity. *Acta Obstet Gynecol Scand* 1996; 75(2): 98–101.
11. Tirado-Gonzalez I, Barrientos G, Tariverdian N, et al. Endometriosis research: animal models for the study of a complex disease. *J Reprod Immunol* 2010; 86(2): 141–147.
12. Defrere S, Van Langendonckt A, Gonzalez Ramos R, et al. Quantification of endometriotic lesions in a murine model by fluorimetric and morphometric analyses. *Hum Reprod* 2006; 21(3): 810–817.
13. Chen QH, Zhou WD, Su ZY, et al. Change of proinflammatory cytokines follows certain patterns after induction of endometriosis in a mouse model. *Fertil Steril* 2010; 93(5): 1448–1454.
14. Umezawa M, Sakata C, Tanaka N, et al. Cytokine and chemokine expression in a rat endometriosis is similar to that in human endometriosis. *Cytokine* 2008; 43(2): 105–109.
15. Rosa-e-Silva JC, Garcia SB, de Sa Rosa-e-Silva AC, et al. Increased cell proliferation in experimentally induced endometriosis in rabbits. *Fertil Steril* 2010; 93(5): 1637–1642.
16. Fazleabas TA. Models of endometriosis: animal models II—non-human primates. In: Giudice LC, Evers JLH and Healy DL (eds) *Endometriosis—science and practice*. 1st ed. Chichester: Wiley Blackwell, 2012, pp. 285–291.
17. Joseph IB, Currie WD and Rawlings NC. Effects of time after ovariectomy, season and oestradiol on luteinizing hormone and follicle-stimulating hormone secretion in ovariectomized ewes. *J Reprod Fertil* 1992; 94(2): 511–523.
18. Culling CFA. Basic staining and mounting procedures. In: Culling CFA (ed.) *Handbook of histopathological and histochemical techniques*. 3rd ed. London: Butterworths and Co., 1974, pp. 192–200.
19. Czernobilsky B and Fox H. Endometriosis. In: Fox H and Wells M (eds) *Obstetrical and gynecological pathology*. 5th ed. London: Elsevier Science Limited, 2003, pp. 963–987.
20. Jacobson VC. The autotransplantation of endometrial tissue in the rabbit. *Arch Surg* 1922; 5(2): 281–300.
21. Schenken RS and Asch RH. Surgical induction of endometriosis in the rabbit: effects on fertility and concentrations of peritoneal fluid prostaglandins. *Fertil Steril* 1980; 34(6): 581–587.
22. Vernon MW and Wilson EA. Studies on the surgical induction of endometriosis in the rat. *Fertil Steril* 1985; 44(5): 684–694.
23. Nap AW. Theories on the pathogenesis of endometriosis. In: Giudice LC, Evers JLH and Healy DL (eds) *Endometriosis—science and practice*. 1st ed. Chichester: Wiley Blackwell, 2012, pp. 42–53.
24. Donnez J, Donnez O, Lousse J-C, et al. Peritoneal, ovarian, and rectovaginal endometriosis are three different entities. In: Giudice LC, Evers JLH and Healy DL (eds) *Endometriosis—science and practice*. 1st ed. Chichester: Wiley Blackwell, 2012, pp. 92–107.
25. Nisolle M and Donnez J. Peritoneal endometriosis, ovarian endometriosis and adenomyotic nodules of the rectovaginal septum are three different entities. *Fertil Steril* 1997; 68(4): 585–596.
26. Czernobilsky B and Morris WJ. A histologic study of ovarian endometriosis with emphasis on hyperplastic and atypical changes. *Obstet Gynecol* 1979; 53(3): 318–323.
27. Mazur TM and Kurman RJ. Endometrial Hyperplasia, Endometrial intraepithelial carcinoma and epithelial cytoplasmic change. In: Mazur TM and Kurman RJ (eds) *Diagnosis of endometrial biopsies and curettings*. 2nd ed. New York: Springer Science, 2005, pp. 178–207.
28. Clement PB, Young RH and Scully RE. Necrotic pseudoxanthomatous nodules of ovary and peritoneum in endometriosis. *Am J Surg Pathol* 1988; 12(5): 390–397.
29. Montag AG, Jenison EL, Griffiths CT, et al. Ovarian clear cell carcinoma: a clinicopathologic analysis of 44 cases. *Int J Gynecol Pathol* 1989; 8(2): 85–96.
30. Lee KR. The pathology of surface epithelial-stromal tumors of the ovary. In: Crum CP and Lee KR (eds) *Diagnostic gynecologic and obstetric pathology*. 1st ed. Philadelphia, PA: Elsevier/Saunders, 2006, pp. 839–903.
31. Sugiyama T and Tsuda H. Clear cell carcinoma of the ovary. In: Reed N, Green JA, Gerhenson DM, et al. (eds) *Rare and uncommon gynecological cancers: a clinical guide*. 1st ed. New York: Springer, 2011, pp. 91–104.